*J Physiol* 587.12 (2009) pp 2903–2918



The Journal of Physiology

# Properties of Orai1 mediated store-operated current depend on the expression levels of STIM1 and Orai1 proteins

N. Scrimgeour[1], T. Litjens[1], L. Ma[1], G. J. Barritt[2] and G. Y. Rychkov[1]

[1] *School of Molecular and Biomedical Science, University of Adelaide, Adelaide, South Australia 5005, Australia*
[2] *Department of Medical Biochemistry, School of Medicine, Flinders University, Adelaide, South Australia 5001, Australia*

**Two cellular proteins, stromal interaction molecule 1 (STIM1) and Orai1, are recently discovered essential components of the $Ca^{2+}$ release activated $Ca^{2+}$ (CRAC) channel. Orai1 polypeptides form the pore of the CRAC channel, while STIM1 plays the role of the endoplasmic reticulum $Ca^{2+}$ sensor required for activation of CRAC current ($I_{CRAC}$) by store depletion. It is not known, however, if the role of STIM1 is limited exclusively to $Ca^{2+}$ sensing, or whether interaction between Orai1 and STIM1, either direct or indirect, also defines the properties of $I_{CRAC}$. In this study we investigated how the relative expression levels of ectopic Orai1 and STIM1 affect the properties of $I_{CRAC}$. The results show that cells expressing low Orai1 : STIM1 ratios produce $I_{CRAC}$ with strong fast $Ca^{2+}$-dependent inactivation, while cells expressing high Orai1 : STIM1 ratios produce $I_{CRAC}$ with strong activation at negative potentials. Moreover, the expression ratio of Orai1 and STIM1 affects $Ca^{2+}$, $Ba^{2+}$ and $Sr^{2+}$ conductance, but has no effect on the current in the absence of divalent cations. The results suggest that several key properties of $Ca^{2+}$ channels formed by Orai1 depend on its interaction with STIM1, and that the stoichiometry of this interaction may vary depending on the relative expression levels of these proteins.**

(Received 10 February 2009; accepted after revision 21 April 2009; first published online 29 April 2009)
**Corresponding author** G. Rychkov: School of Molecular and Biomedical Science, University of Adelaide, Adelaide, South Australia, 5005, Australia. Email: grigori.rychkov@adelaide.edu.au

**Abbreviations** 2-APB, 2-aminoethoxydiphenyl borate; CAD, CRAC activation domain; CRAC, $Ca^{2+}$-release activated $Ca^{2+}$; DVF, divalent free; eGFP, enhanced green fluorescent protein; ER, endoplasmic reticulum; $I_{CRAC}$, $Ca^{2+}$-release activated $Ca^{2+}$ current; $Ins_3P$, inositiol 1,4,5-trisphosphate; $I_{SOC}$, store operated $Ca^{2+}$ current; $I$–$V$, current–voltage; GFP, green fluorescent protein; RBL, rat basophilic leukaemia; SCID, severe combined immunodeficiency syndrome; siRNA, short interfering RNA; SOCE, store operated $Ca^{2+}$ entry; STIM1, stromal interaction molecule 1.

A two decade long search for the molecular components of store-operated $Ca^{2+}$ entry (SOCE) and $Ca^{2+}$ release activated $Ca^{2+}$ (CRAC) channel in particular has been rewarded by the discovery of two cellular proteins, stromal interaction molecule 1 (STIM1) and Orai1 (Liou *et al.* 2005; Roos *et al.* 2005; Zhang *et al.* 2005; Feske *et al.* 2006; Vig *et al.* 2006*b*). STIM1 is localised both on the plasma membrane and the endoplasmic reticulum (ER) (Manji *et al.* 2000; Liou *et al.* 2005; Spassova *et al.* 2006). STIM1 that is expressed in the ER plays the role of the $Ca^{2+}$ sensor in the ER lumen, while Orai1 is expressed on the plasma membrane and contributes to the $Ca^{2+}$ selective pore of the channel (Prakriya *et al.* 2006; Taylor, 2006; Yeromin *et al.* 2006; Putney, 2007). Knockdown of either STIM1 or Orai1 by siRNA leads to a suppression of the native $I_{CRAC}$ in hematopoietic and other cell types, and a missense mutation in the gene encoding Orai1 has been linked to one form of hereditary severe combined immune deficiency (SCID) syndrome, associated with a reduced SOCE in lymphocytes (Roos *et al.* 2005; Feske *et al.* 2006; Litjens *et al.* 2007; Luik & Lewis, 2007). Ectopic expression of either STIM1 or Orai1 alone has little effect on the amplitude of the native $I_{CRAC}$, but ectopic expression of both proteins together produces a large store-operated $Ca^{2+}$ current with properties very similar to those of $I_{CRAC}$ (Roos *et al.* 2005; Peinelt *et al.* 2006; Soboloff *et al.* 2006; Vig *et al.* 2006*b*).

Present understanding of the SOCE mechanism suggests that depletion of intracellular $Ca^{2+}$ stores causes STIM1 to accumulate in junctional ER, which is located in close proximity to the plasma membrane, while Orai1 accumulates in the areas of plasma membrane apposed STIM1 puncta (Luik *et al.* 2006; Varnai *et al.* 2007). Interaction between STIM1 and Orai1, either direct through cytoplasmic coiled-coil regions, or indirect through other binding partners results in activation of


DOI: 10.1113/jphysiol.2009.170662

$Ca^{2+}$ entry (Huang *et al.* 2006; Li *et al.* 2007; Varnai *et al.* 2007; Muik *et al.* 2008). Accumulation of STIM1 into puncta near the plasma membrane is essential for activation of the current through the channels formed by the Orai1 peptides, and reversal of STIM1 localisation by either replenishment of $Ca^{2+}$ stores, or pharmacologically, terminates $Ca^{2+}$ entry (Smyth *et al.* 2008).

Site-directed mutagenesis has been used to confirm basic functions and to localise some functionally important regions of STIM1 and Orai1. Several mutations in the putative EF-hand $Ca^{2+}$-sensing domain of STIM1 have been shown to produce constitutively active $Ca^{2+}$ currents, confirming that STIM1 is the $Ca^{2+}$ sensor that communicates the filling state of $Ca^{2+}$ stores to the plasma membrane (Zhang *et al.* 2005; Spassova *et al.* 2006). The observation that mutations of several acidic residues in Orai1 result in significant changes in the selectivity of Orai1/STIM1 mediated current supported the notion that Orai1 forms the pore of the CRAC channel (Prakriya *et al.* 2006; Vig *et al.* 2006*a*; Yeromin *et al.* 2006). Recent investigations of the stoichiometry of the Orai1 pore and stoichiometry of interaction between Orai1 and STIM1 suggested that the pore of the channel is formed by two Orai1 dimers, while two STIM1 peptides are required for activation of one channel (Mignen *et al.* 2008; Ji *et al.* 2008; Penna *et al.* 2008). It is not yet clear, however, whether 4 Orai1 : 2 STIM1 is the only stoichiometry that produces a functional channel, and whether STIM1, apart from being $Ca^{2+}$ sensor in the ER, plays any role in defining the properties of the Orai1 mediated current.

In the present study we expressed Orai1 and STIM1 at various ratios in a heterologous expression system and investigated the properties of the resulting store-operated currents. Transfection of H4IIE liver cells with STIM1 and Orai1 plasmids mixed in different proportions revealed that cells transfected with an excess of STIM1 were more likely to express currents showing fast $Ca^{2+}$-dependent inactivation, while cells transfected with an excess of Orai1 produced currents that showed little inactivation, or even activation at negative potentials. Furthermore, expression ratios of Orai1 and STIM1 affected $Ca^{2+}$, $Ba^{2+}$ and $Sr^{2+}$ conductance and potentiation of the currents by 2-APB. This suggests that some key properties of Orai1/STIM1 mediated currents that have been used to identify $I_{CRAC}$ in the past, including the kinetics of fast $Ca^{2+}$ dependent inactivation, arise from interaction between STIM1 and Orai1 and can not be attributed to Orai1 alone.

## Methods

### Cell culture and transfections

H4IIE (ATCC CRL 1548) cells and HEK293 cells were cultured at 37°C in 5% (v/v) $CO_2$ in air in Dulbecco's modified Eagle's medium (DMEM) supplemented with 100 $\mu$M minimal essential medium (MEM) non-essential amino acids, 2 mM L-glutamine and 10% (v/v) fetal bovine serum (FBS) (complete DMEM). To express Orai1 and STIM1 proteins, H4IIE cells growing on glass coverslips at a 10–20% density were transfected using PolyFect transfection reagent (Qiagen, Germany) according to the manufacturer specifications.

### Subcloning of STIM1 and Orai1

Full-length cDNAs for hOrai1 (NM_032790) and hSTIM1 (NM_003156) were purchased from OpenBioSystems (Huntsville, AL, USA). The Orai1 and STIM1 open reading frames were then PCR amplified and subcloned into the expression vector pCMV-Sport6 (OpenBioSystems) and the green fluorescent protein (GFP)-coexpresssing vector pAdTrack-CMV (a gift from Drs Lei Zhang and S. Brookes, Flinders University, Adelaide). The GFP fused Orai1 and STIM1 were expressed from constructs pEX-GFP-Myc-Orai1 (a gift from Prof. R. Lewis and Dr. R. Dolmetsch, Stanford University, USA) and pApuro-GFP-STIM1 (a gift from Dr. T. Kurosaki, Research Centre for Allergy and Immunology, Kanagawa, Japan), respectively. Integrity of the constructs was verified by DNA sequencing.

### Western blotting

HEK293 cells transfected with pEX-GFP-Myc-Orai1 and pApuro-GFP-STIM1 were harvested and incubated on ice for 30 min in the lysis buffer containing 150 mM NaCl, 50 mM Tris-HCl (pH 7.4), 1 mM EDTA (pH 8.2), 0.25% sodium deoxycholate, 1% NonIdet P-40, 0.1% SDS and 0.1% protease inhibitor cocktail (Sigma). The concentration of crude proteins was measured using the BCA Protein Determination Kit (Sigma). Equal amounts of protein were separated on 10% SDS-PAGE and transferred to nitrocellulose membranes. The blots were then blocked for 1 h in Tris-buffered saline with Tween-20 (TBST) buffer (150 mM NaCl, 25 mM Tris, pH 7.4, 0.1% Tween-20) containing 5% non-fat milk powder and incubated in the blocking solution for 1 h with the appropriate primary antibody, including anti-STIM1 monoclonal antibody (1 : 1000 diluted, BD Biosciences), anti-GFP polyclonal antibody Ab290 (1 : 10 000 diluted, Abcam) and anti-GAPDH (1 : 500 diluted, Santa Cruz Biotechnology, Inc., Santa Cruz, CA, USA). After four washes in TBST buffer and 1 h incubation with the secondary antibodies (horseradish peroxidase-conjugated anti-mouse IgG (1 : 5000 diluted, Sigma) or anti-Rabbit IgG (1 : 1000 diluted, Rockland Immunochemicals Inc., Gilbertsville, PA, USA)) the protein bands were visualised with an enhanced chemiluminescence detection system (Amersham Biosciences/GE Healthcare). The

autoradiographs were scanned using a GS-800 densitometer (Bio-Rad Laboratories, Hercules, CA, USA) and the band intensities quantified using Quantity One software version 4.3.1 (Bio-Rad Laboratories).

### Patch clamping

Whole-cell patch clamping was performed at room temperature using a computer-based patch-clamp amplifier (EPC-9, HEKA Electronics, Germany) and PULSE software (HEKA Elektronik, Lambrecht/Pfalz, Germany). The bath solution contained (mM): NaCl, 140; CsCl, 4; $CaCl_2$, 10; $MgCl_2$, 2; glucose 10; and Hepes, 10; adjusted to pH 7.4 with NaOH. The internal solution contained (mM): caesium glutamate, 130; $CaCl_2$ 5; $MgCl_2$ 5; MgATP 1; EGTA, 10; and Hepes, 10; adjusted to pH 7.2 with NaOH. The calculated internal free $Ca^{2+}$ concentration was about 100 nM (EQCAL, Biosoft, Cambridge, UK). Depletion of the intracellular $Ca^{2+}$ stores was achieved by addition of 20 $\mu$M $InsP_3$ (Amersham) to the internal solution. Patch pipettes were pulled from borosilicate glass and fire-polished; pipette resistance ranged between 3 and 5 MΩ. Series resistance did not exceed 10 MΩ and was compensated by 50–70%. In order to monitor the development of $I_{SOC}$, 100 ms voltage ramps between −138 and +102 mV were applied every 2 s, starting immediately after achieving the whole-cell configuration. Acquired currents were filtered at 2.7 kHz and sampled at 10 kHz. All voltages shown have been corrected for the liquid junction potential of −18 mV between the bath and electrode solutions (estimated by JPCalc; Barry, 1994). The holding potential was −18 mV throughout. Cell capacitance was compensated automatically by the EPC9 amplifier.

### Data analysis

Normalised instantaneous tail currents for voltage steps to −118 mV after test pulses in the range of −158 to 102 mV were used to produce the apparent open probability ($P_o$) curves by fitting with the Boltzmann distribution with an offset of the form:

$$P_o(V) = P_{min} + \frac{1 - P_{min}}{1 + \exp((V_{1/2} - V)/k)} \quad (1)$$

where $P_{min}$ is an offset, $V$ is the membrane potential, $V_{1/2}$ is the half-maximal activation potential, and $k$ is the slope factor.

To determine the amplitude of the instantaneous tail currents and to minimise the error due to the cell capacitance, the tail currents were fitted with a single exponential function to the beginning of the −118 mV pulse.

To obtain bell-shaped apparent $P_o$ curves to fit some of the experimental data, we used a multiple of two Boltzmann distributions with independent parameters:

$$P_o(V) = P_o^1(V) \times P_o^2(V) \quad (2)$$

Where $P_o^1(V)$ and $P_o^2(V)$ are independent Boltzmann distributions of the form shown by eqn (1). Equation (1) assumes that there is a voltage-dependent gate present in the channel, while eqn (2) assumes the presence of two such voltage-dependent gates independent of each other. Nether of these statements is necessarily correct for the channel under study, as voltage dependence of the open probability does not necessarily imply presence of a voltage sensor in the channel. Nevertheless, these equations provide the means for quantitative description of the data.

## Results

### Ectopic expression of Orai1 and STIM1 in H4IIE liver cells

In order to investigate the properties of the heterologously expressed Orai1/STIM1 mediated current, we co-transfected plasmids containing STIM1 and Orai1 cDNA at a 1 : 1 ratio into H4IIE liver cells. To facilitate identification of the transfected cells, either the STIM1 or Orai1 plasmid contained cDNA encoding enhanced green fluorescent protein (eGFP). The time course of activation of Orai1/STIM1 mediated currents varied between transfected cells, with some cells showing no constitutively active currents and relatively slow activation by intracellular $InsP_3$ (Fig. 1*A*, cell 1), while others showed very large initial currents that inactivated to a steady state (Fig. 1*A*, cell 4). The majority of transfected cells showed intermediate patterns, with some exhibiting a constitutively active current (Fig. 1*A*, cells 2 and 3). The presence of an apparently constitutively active current at the start of the recording could be a result of very fast activation, within 2–3 s of achieving whole cell configuration, due to $InsP_3$ diffusing from the pipette. However, when transfected cells were patched with a pipette containing no $InsP_3$ and $Ca^{2+}$ buffered to 120 nM, a constitutively active current was still present in a high proportion of cells (∼30%, not shown), suggesting that fast diffusion of $InsP_3$ is an unlikely explanation. Similar constitutively active Orai1/STIM1 currents were reported in a recent study (Zhang *et al.* 2008).

The *I–V* plots in all transfected cells showed strong inward rectification and very positive reversal potential, similar to that reported in other studies with ectopic expression of Orai1 and STIM1 (Peinelt *et al.* 2006; Soboloff *et al.* 2006). The shape of *I–V* plots varied between cells, with some showing stronger inward

rectification at potentials below −100 mV than others (Fig. 1*B*).

Further experiments showed that the variation in the shape of the *I–V* plots recorded from different cells was caused by the variations in the fast $Ca^{2+}$-dependent inactivation of the currents at negative potentials. Thus we observed cells with very strong fast $Ca^{2+}$ dependent inactivation (Fig. 1*Ca*), cells with very little or no inactivation (Fig. 1*Cc*), and all stages in between (Fig. 1*Cb*). Such variations in the kinetics of Orai1/STIM1 mediated currents suggest that fast $Ca^{2+}$ dependent inactivation is not an intrinsic property that can be ascribed to Orai1 alone, otherwise it would be very similar in all transfected cells. Rather, the results suggest that inactivation arises from interaction of Orai1 with some other protein in the cell, the amount of which varies from cell to cell. The obvious candidate for such a protein that interacts with Orai1 and changes the kinetics of the current is STIM1.

To investigate this possibility we varied the ratio between the plasmids in the transfection mixture in order to change the relative amounts of expressed Orai1 and STIM1 proteins in the cell. First, the amount of STIM1 plasmid in the transfection mixture was kept constant at 0.4 pmol and the amount of the plasmid containing Orai1 varied between 0.05 and 0.8 pmol. Subsequently, the amount of Orai1 plasmid in the transfection mixture was kept constant at 0.4 pmol and the amount of the plasmid containing STIM1 varied between 0.2 and 1.2 pmol. The volume of the transfection mixture was kept constant in all transfections. To compare inactivation of Orai1/STIM1 currents

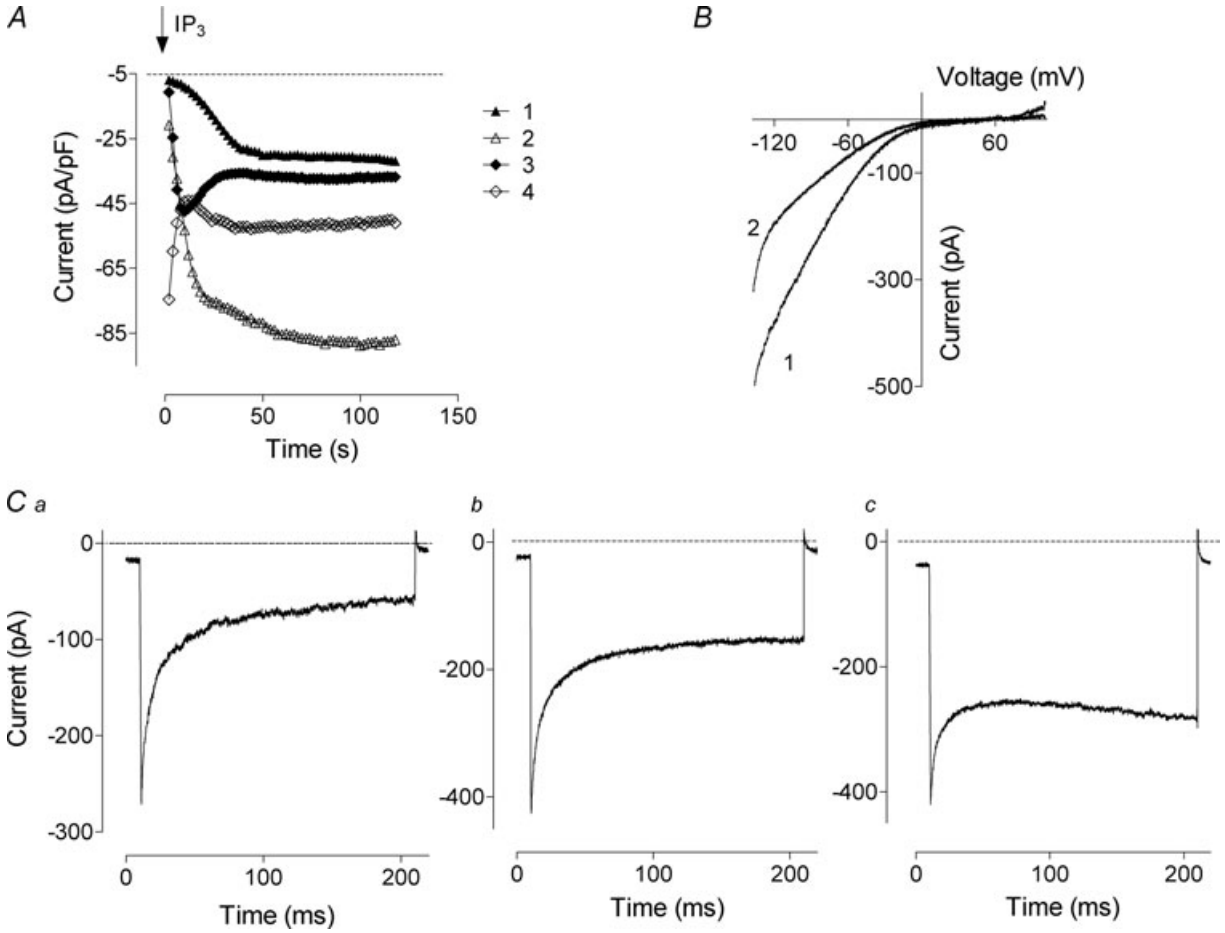


**Figure 1. Overexpression of STIM1 and Orai1 in H4IIE cells**
*A*, examples of development of the Orai1/STIM1 mediated current. Each point represents the amplitude of the current at −118 mV measured from the responses to voltage ramps ranging from −138 mV to 102 mV and applied every 2 s. *B*, examples of the *I–V* plots obtained from cells expressing both STIM1 and Orai1. *C*, examples of the currents obtained in response to 200 ms steps to −138 mV. Traces were taken 40–60 s after obtaining whole-cell configuration when the amplitude of the current reached steady-state. Note significant variations in current kinetics. Cells were transfected with Orai1/STIM1 in a molar ratio of 1 : 1. Leakage was determined by applying 50 $\mu$M 2-APB at the end of the experiment and was corrected for in panels *B* and *C*, but not *A*.

recorded from different cells, similar to those shown in Fig. 1*C*, we normalised amplitude of the current at the end of a 200 ms, −100 mV pulse ($I_{200}$) to the amplitude of the current at the beginning of the pulse ($I_0$). In cells transfected with 0.4 pmol STIM1 and 0.4 pmol Orai1 plasmids (1 : 1 ratio) the average extent of inactivation ($I_{200}/I_0$) was $0.80 \pm 0.06$ ($n = 13$) (Fig. 2*A*), although inactivation varied significantly between individual cells. With decreasing concentration of Orai1 plasmid in the transfection mixture, the inactivation became more pronounced and the variability between cells reduced. At the ratio of 1 : 8 (0.05 pmole Orai1/0.4 pmol STIM1) all cells produced inactivating currents with an average $I_{200}/I_0$ of $0.46 \pm 0.03$ ($n = 7$) (Fig. 2*A*). Similarly, the inactivation became more pronounced when the concentration of Orai1 plasmid was kept constant and the concentration of STIM1 plasmid increased (Fig. 2*B*). Comparison of the results obtained with different amounts of each plasmid revealed that the extent of inactivation depended on the ratio between the amounts of the plasmids, but not on their absolute amounts (Fig. 2*A*, *B*).

In these experiments, we have found that more consistent results were obtained if the plasmid containing the GFP sequence was in excess. Therefore, in all subsequent experiments we transfected cells with mixtures of 1 : 2 or 1 : 4 Orai1/(STIM1 + GFP) and 2 : 1 or 4 : 1 (Orai1 + GFP)/STIM1 to investigate the properties of inactivating and non-inactivating currents, respectively.

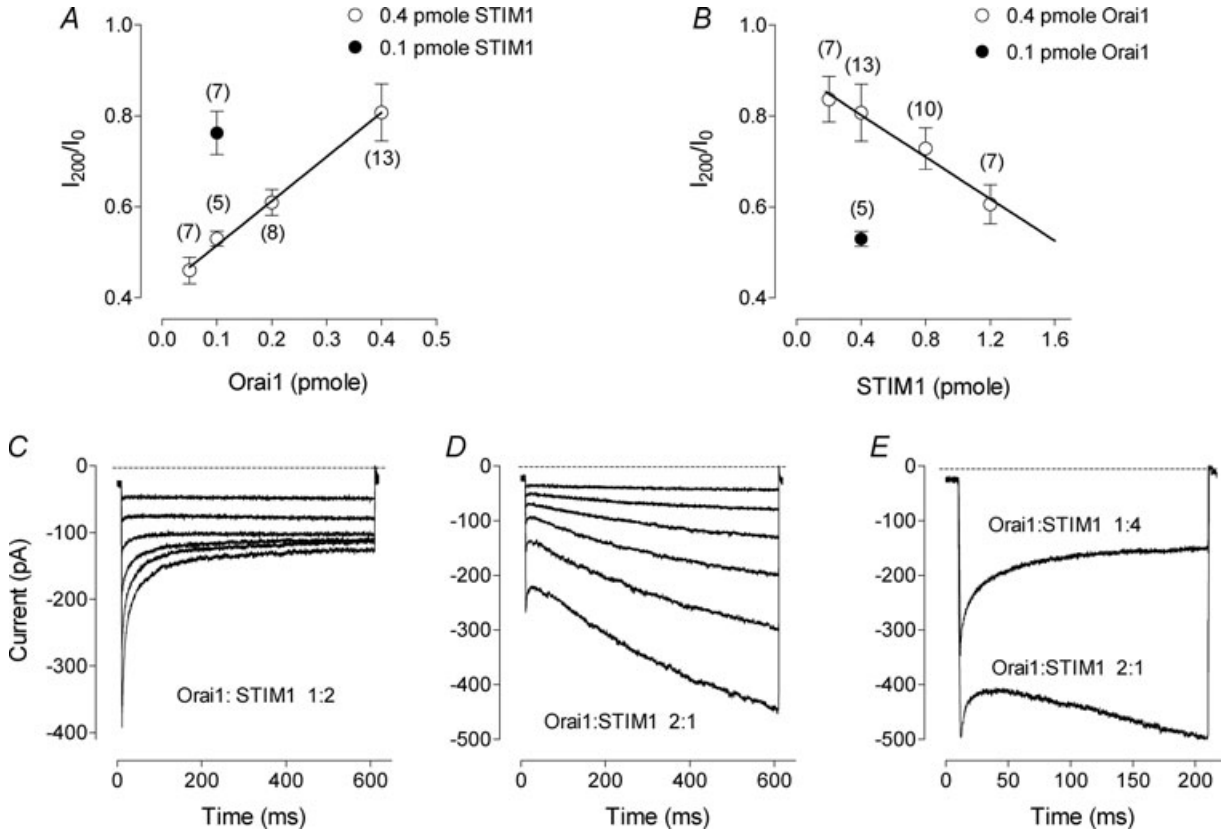


**Figure 2. The kinetics of the Orai1/STIM1 mediated current under different transfection conditions**
*A*, dependence of the inactivation at negative potentials on the amount of the Orai1 plasmid. Each point represents the relative amplitude of the Orai1/STIM1 mediated current at the end of the 200 ms step to −118 mV ($I_{200}$) normalised to the peak current at the beginning of the step ($I_0$). Open circles represent averaged data for the 0.4 pmol of STIM1. For comparison, the averaged data for 0.1 pmol STIM1 and 0.1 pmol Orai1 is presented (filled circle). Number of cells is indicated in brackets. Note that the extent of the current inactivation in the cells transfected with 0.1 pmol STIM1 and 0.1 pmol Orai1 is not different from that in cells transfected with 0.4 pmol STIM1 and 0.4 pmol Orai1 ($P = 0.6$). Continuous line represents linear regression for the data obtained with the range of Orai1 concentrations and 0.4 pmol STIM1 ($r^2 = 0.48$; $P < 0.0001$). *B*, dependence of the inactivation at negative potentials on the amount of the STIM1 plasmid. Continuous line represents linear regression for the data obtained with the range of STIM1 concentrations and 0.4 pmol Orai1 ($r^2 = 0.98$; $P < 0.01$). *C*, example of the currents recorded from a cell transfected with 1 Orai1/2 (STIM1+GFP) mixture. *D*, example of the currents recorded from a cell transfected with 2 (Orai1+GFP)/1 STIM1 mixture. Current traces were obtained in response to 600 ms steps ranging from −138 mV to −38 mV in 20 mV increments. *E*, example of the currents obtained in HEK293 cells using similar transfection mixtures.

Examples of such currents are shown in Fig. 2*C* and *D*. With longer hyperpolarising pulses, most cells transfected with an excess of Orai1 showed strongly activating currents at negative potentials (Fig. 2*D*).

We have shown previously that H4IIE cells express $I_{SOC}$ with properties virtually identical to those of $I_{CRAC}$ in hematopoietic cells (Litjens *et al.* 2004; Aromataris *et al.* 2008). The amplitude of the native $I_{SOC}$ in H4IIE cells ($\sim$2.5 pA pF$^{-1}$ at $-$118 mV) is at least severalfold smaller than the amplitude of the currents mediated by ectopically expressed Orai1/STIM1 (15–60 pA pF$^{-1}$). Therefore, the presence of native STIM1 and Orai in H4IIE cells was unlikely to have a significant impact on the results. Nevertheless, to investigate the possibility that the kinetics of the currents mediated by ectopically expressed Orai1/STIM1 was influenced by the presence of the endogenous $I_{SOC}$ or some other proteins in H4IIE cells we used HEK293 cells, which have very small native $I_{SOC}$ (Mercer *et al.* 2006; Soboloff *et al.* 2006). Similarly to H4IIE cells, HEK293 cells produced inactivating currents when transfected with an excess of STIM1 and activating currents when transfected with an excess of Orai1 (Fig. 2*E*). Furthermore, results similar to those shown in Fig. 2*B*, *C* and *D* were obtained using plasmids containing GFP fused Orai1 and STIM1 (GFP-Orai1 and GFP-STIM1, not shown).

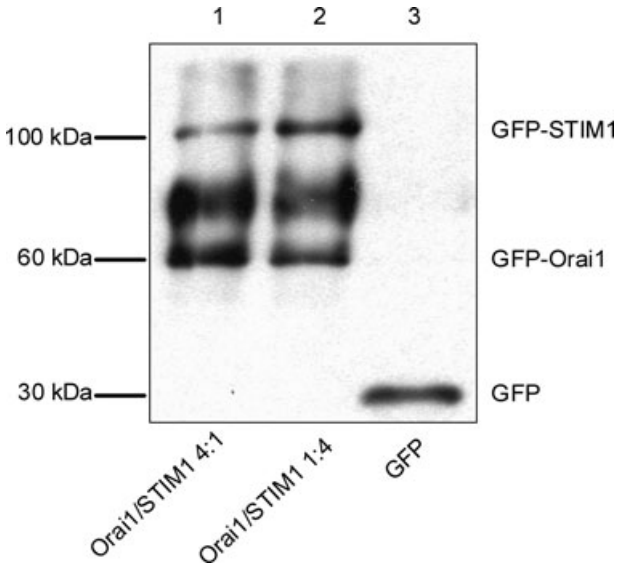


**Figure 3. Western blotting of the expressed GFP-labelled Orai1 and STIM1**
Each lane was loaded with lysates (2 $\mu$g of protein) of HEK293 cells transfected with GFP-Orai1 and GFP-STIM1 containing plasmids at a molar ratio of 4 : 1 (lane 1); GFP-Orai1 and GFP-STIM1 containing plasmids at a molar ratio of 1 : 4 (lane 2); or GFP alone containing plasmid (lane 3). The blot was probed with anti-GFP antibody. The relative amounts of the expressed Orai1 and STIM1 proteins in the same transfection and between transfections were estimated by measuring optical densities of the corresponding bands ($n = 3$).

In the next set of experiments we transfected HEK293 cells with GFP-STIM1 and GFP-Orai1, and used Western blots probed with anti-GFP to estimate the relative amounts of the STIM1 and Orai1 proteins expressed under the transfection conditions used in patch clamping. GFP-STIM1 appeared on a Western blot as a clear single band above 100 kDa (Fig. 3). The same single band was obtained if we used anti-STIM1 (not shown). GFP-Orai1, however, appeared as a double band above 60 kDa (Fig. 3). The wide band of higher molecular weight for GFP-Orai1 was likely to be the result of post-translational modification of Orai1 (glycosylation) (Gwack *et al.* 2007). On average, the intensities of the bands corresponded well with the amounts of the transfected plasmids. For the 4 Orai1 : 1 STIM1 transfection (Fig. 3, first lane) the intensity ratio between the GFP-Orai1 single band of lower molecular weight and the GFP-STIM1 band was $5.75 \pm 0.47$ ($n = 3$), while for the 1 Orai1 : 4 STIM1 transfection (Fig. 3, second line) this ratio was $0.48 \pm 0.01$ ($n = 3$).

A fourfold increase in the amount of a plasmid in the transfection mixture resulted in $3.65 \pm 0.13$ and $3.21 \pm 0.27$ ($n = 3$)-fold increase of GFP-STIM1 and GFP-Orai1 expression respectively (Fig. 3). Similar results for STIM1 were obtained when anti-STIM1 was used instead of anti-GFP (not shown). These results demonstrate that variations in the amounts of the STIM1 and Orai1 containing plasmids in the transfection mixtures were closely followed by the changes in the expression levels of the corresponding proteins.

### $Ca^{2+}$ dependence of the amplitude and kinetics of the Orai1/STIM1 mediated currents

Reduction of the $Ca^{2+}$ concentration in the bath solution from 10 to 2 mM resulted in the reduction of the amplitude by about 55% for both activating (4 : 1 Orai1/STIM1 ratio) and inactivating (1 : 4 Orai1/STIM1 ratio) Orai1/STIM1 mediated current (Fig. 4*A* and *B*). Increase of the $Ca^{2+}$ concentration to 50 mM caused a sharp increase in the amplitude which was followed by an exponential decline. A further increase to 100 mM resulted in a small potentiation and further decline in the amplitude. Upon return to 10 mM $Ca^{2+}$ the amplitude of the current was reduced and then slowly returned to the initial level. Qualitatively, dependence of the amplitude of inactivating and activating currents on $Ca^{2+}$ concentration was similar and could be explained by slow feedback inhibition of the channel by $Ca^{2+}$ entering the cell. Similar slow $Ca^{2+}$-dependent inhibition has been previously described for $I_{CRAC}$ in lymphocytes (Zweifach & Lewis, 1995*b*). Quantitatively, however, the steady state amplitudes of the activating current in 50 mM and 100 mM $Ca^{2+}$ were significantly larger than that in 10 mM $Ca^{2+}$; while the steady state

amplitudes of the inactivating current in 50 mM and 100 mM $Ca^{2+}$ were significantly lower (Fig. 4*A* and *B*). The initial potentiation, both relative and absolute, of the current by higher $Ca^{2+}$ concentrations was also significantly stronger for activating currents.

In the next experiment we compared $Ca^{2+}$ dependence of the currents on a much shorter time scale. As expected, the kinetics and the extent of the fast $Ca^{2+}$-dependent inactivation of the currents recorded from cells transfected with an excess of STIM1 were strongly dependent on the external $Ca^{2+}$ concentration, similarly to that of native $I_{SOC}$ in H4IIE cells or $I_{CRAC}$ in hematopoietic cells (Fig. 4*C*) (Zweifach & Lewis, 1995*a*; Litjens *et al.* 2004) . At higher $Ca^{2+}$ concentrations the inactivation was faster and more complete. In contrast, the kinetics of activating currents recorded from cells transfected with an excess of Orai1 showed no dependence on the external $Ca^{2+}$ concentration between 2 and 100 mM (Fig. 4*D*).

### Selectivity for $Ba^{2+}$ and $Sr^{2+}$

In cells transfected with an excess of Orai1 (4 : 1 Orai1/STIM1 ratio) that produced activating currents, replacement of $Ca^{2+}$ with $Ba^{2+}$ or $Sr^{2+}$ in the bath solution led to a decrease of the current amplitude. On average, at −100 mV, $Ba^{2+}$ current was ∼70% smaller than the $Ca^{2+}$ current. Current carried by $Sr^{2+}$ at −100 mV was ∼35% smaller than $Ca^{2+}$ current (Fig. 5*A*). In the cells

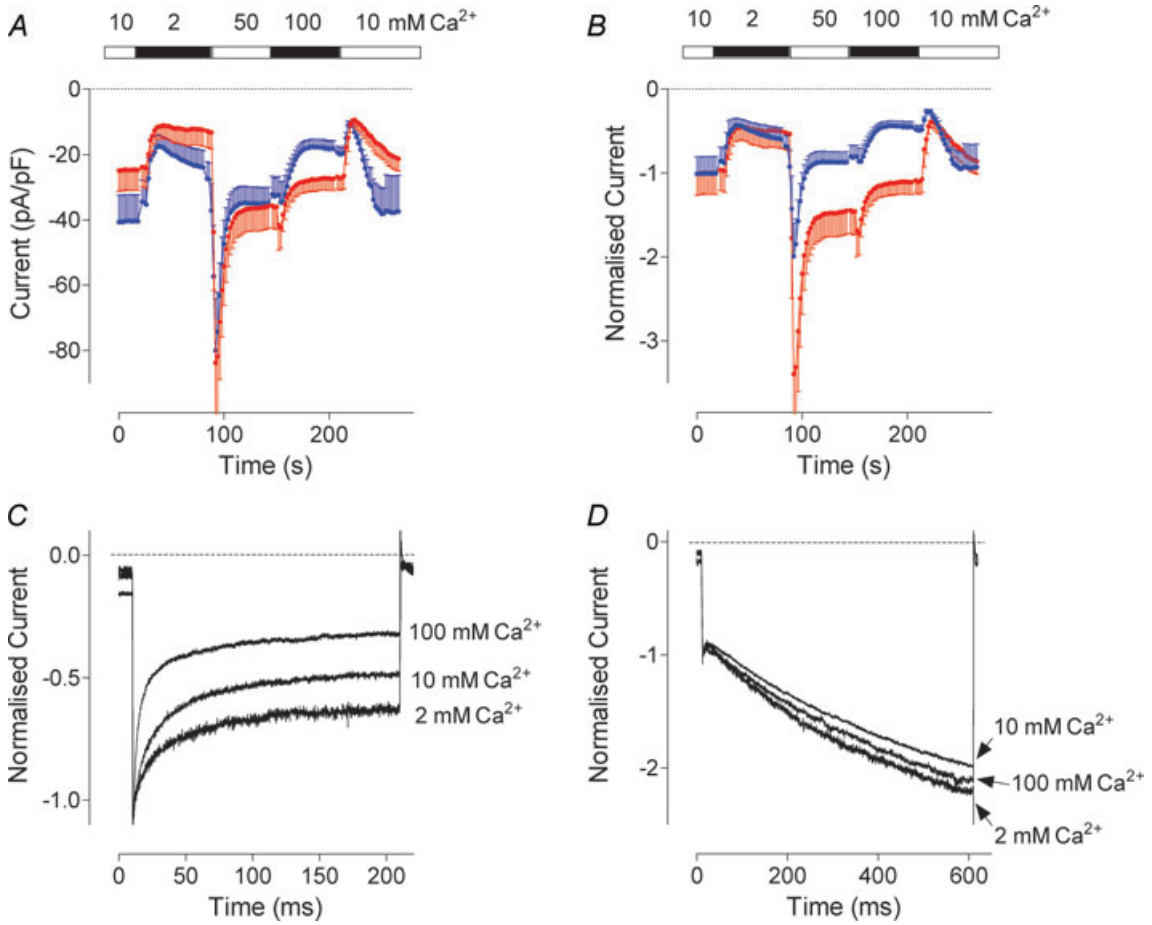


**Figure 4. Dependence of the Orai1/STIM1 current on the external $Ca^{2+}$ concentration**
*A*, amplitude of the Orai1/STIM1 mediated current at −118 mV at different $Ca^{2+}$ concentrations. Data were obtained in cells transfected with Orai1 and STIM1 plasmids at a molar ratio of either 4 : 1 (blue trace) or 1 : 4 (red trace). Each point represents the amplitude of the current at −118 mV measured from the responses to voltage ramps ranging from −138 mV to 102 mV and applied every 2 s. Zero-time point on panels *A* and *B* corresponds to 60 s after obtaining whole cell configuration. *B*, the same data as in panel *A* normalised to the current amplitude in 10 mM $Ca^{2+}$. *C* and *D*, dependence of current kinetics on the external $Ca^{2+}$ concentration. All traces are recorded in response to voltage steps to −118 mV and normalised to the current amplitude at the beginning of the pulse. Traces were taken 30–40 s after changing $Ca^{2+}$ concentration in the bath when the amplitude of the current reached steady-state (see panel *A*).

transfected with an excess of STIM1 (1 : 4 Orai1/STIM1 ratio) and producing inactivating currents, replacement of $Ca^{2+}$ with $Ba^{2+}$ or $Sr^{2+}$ in the bath solution led to instantaneous reduction in the current amplitude followed by its gradual increase. On average, at −100 mV, $Ba^{2+}$ current was just 10% smaller than the $Ca^{2+}$ current, while current carried by $Sr^{2+}$ at −100 mV was ∼40% larger than $Ca^{2+}$ current (Fig. 5*A*). The shape of the *I–V* plots obtained in response to voltage ramps in the presence of $Ba^{2+}$ and $Sr^{2+}$ suggested a reduced open probability of the channel at holding potential and activation of the current by hyperpolarisation (Fig. 5*B*). This was confirmed by applying voltage steps to −100 mV (Fig. 5*C*). Replacement of $Ca^{2+}$ with $Ba^{2+}$ or $Sr^{2+}$ in cells expressing either inactivating or activating $Ca^{2+}$ currents produced currents activated by hyperpolarisation. The kinetics of the current activation at −100 mV in the presence of $Ba^{2+}$ was significantly faster in cells with inactivating $Ca^{2+}$ currents (Fig. 5*C*).

### Voltage dependence of open probability

The change in the current kinetics from inactivating to activating suggests a change in the voltage dependence of the open probability of the channel. To quantify the relative open probability of the expressed channels under different conditions we used peak tail currents at −100 mV (see Methods, Fig. 6). In cells transfected with an excess of STIM1 and showing inactivating $Ca^{2+}$ currents, the maximum open probability was at 0 mV and above, while the relative minimum open probability saturated

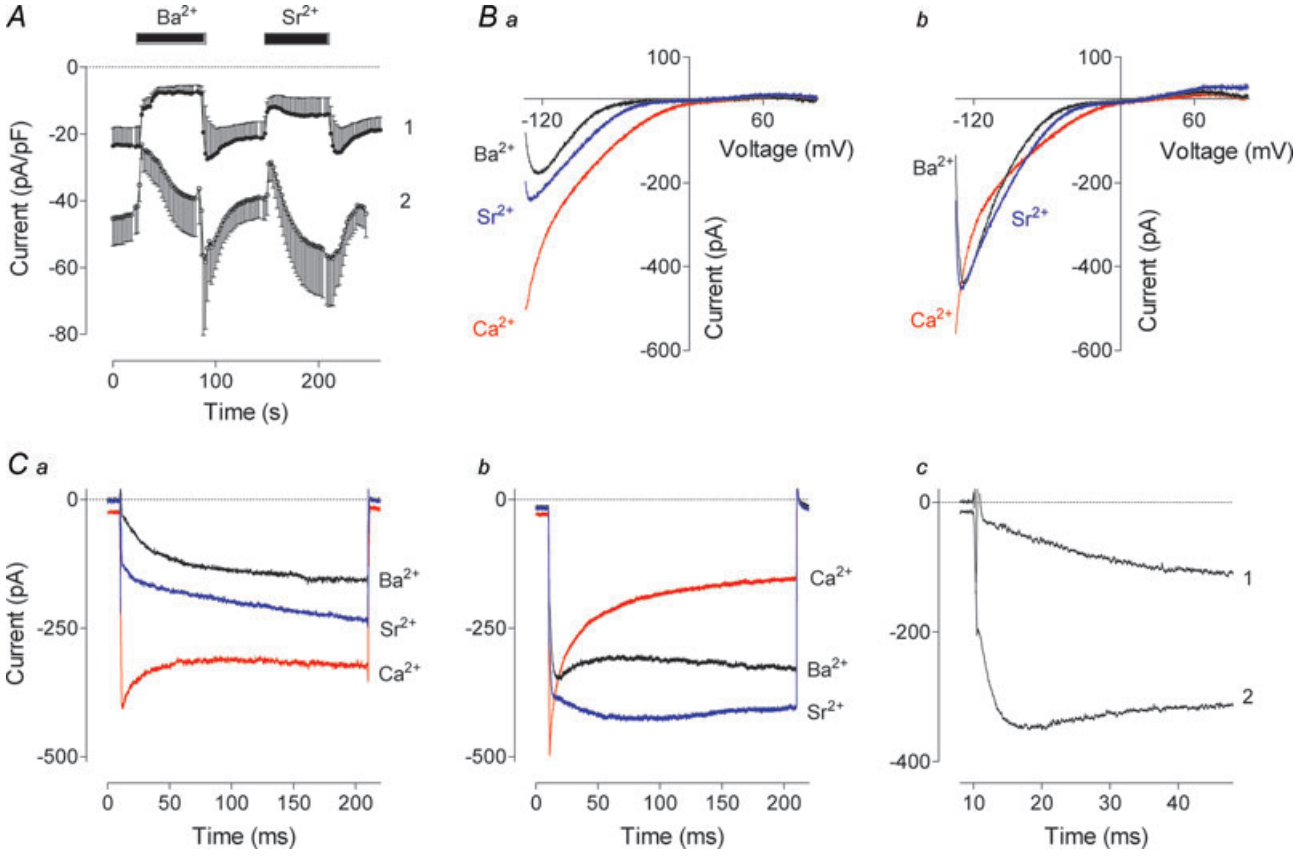


**Figure 5. Effects of $Ba^{2+}$ and $Sr^{2+}$ on the Orai1/STIM1 currents obtained under different transfection conditions**

*A*, dependence of the amplitude of the Orai1/STIM1-mediated current at −118 mV on $Ba^{2+}$ and $Sr^{2+}$. Data were obtained in cells transfected with Orai1 and STIM1 plasmids at a molar ratio of either 4 : 1 (trace 1) or 1 : 4 (trace 2). Each point represents the amplitude of the current at −118 mV measured from the responses to voltage ramps ranging from −138 mV to 102 mV and applied every 2 s. Zero-time point corresponds to 60 s after achieving whole cell. *B*, representative *I–V* plots of the data shown on panel *A*. *a* corresponds to trace 1, and *b* corresponds to trace 2 on panel *A*. *C*, representative current traces in response to steps to −118 mV of the data shown on panel *A*. *a* corresponds to trace 1, and *b* corresponds to trace 2 on panel *A*. *c*, the same $Ba^{2+}$ traces as shown on panels *a* and *b* but on a shorter time scale. Traces shown on panels B and C were taken 40–60 s after applying $Ba^{2+}$ or $Sr^{2+}$ in the bath.

at about 0.25 at potentials below −140 mV (Fig. 6*A*). The normalised amplitude of the peak tail currents plotted against voltage could be fitted with a single Boltzmann function (see Methods). Increasing the length of the voltage steps from 100 ms to 600 ms in these cells did not reveal any other type of voltage dependence of the current and did not shift the Boltzmann curve (not shown). The half-maximum activation voltage was −72 mV and the slope of the curve corresponded to a gating charge of approximately −1.

In cells expressing activating $Ca^{2+}$ currents, the amplitude of the peak tail currents at −100 mV showed complex dependence on the voltage of the preceding steps. In general, relative open probability of activating currents showed bell-shaped voltage dependence between −120 and 80 mV with a maximum at about −30 mV (Fig. 6*B–D*). The voltage dependence of the open probability between −140 mV and −20 mV was very similar to that of the inactivating $Ca^{2+}$ currents and presumably was due to the same gating process, while the open probability between −20 and 80 mV had the opposite voltage dependence (Fig. 6*C*). The data points could be well fitted with a multiple of two independent Boltzmann functions (eqn (2), Methods). Slight upward deviation of the points obtained after the steps to 100 and 120 mV could be due to a poor fit of very fast tail currents, or due to the activity of some native channels present in H4IIE cells at these potentials.

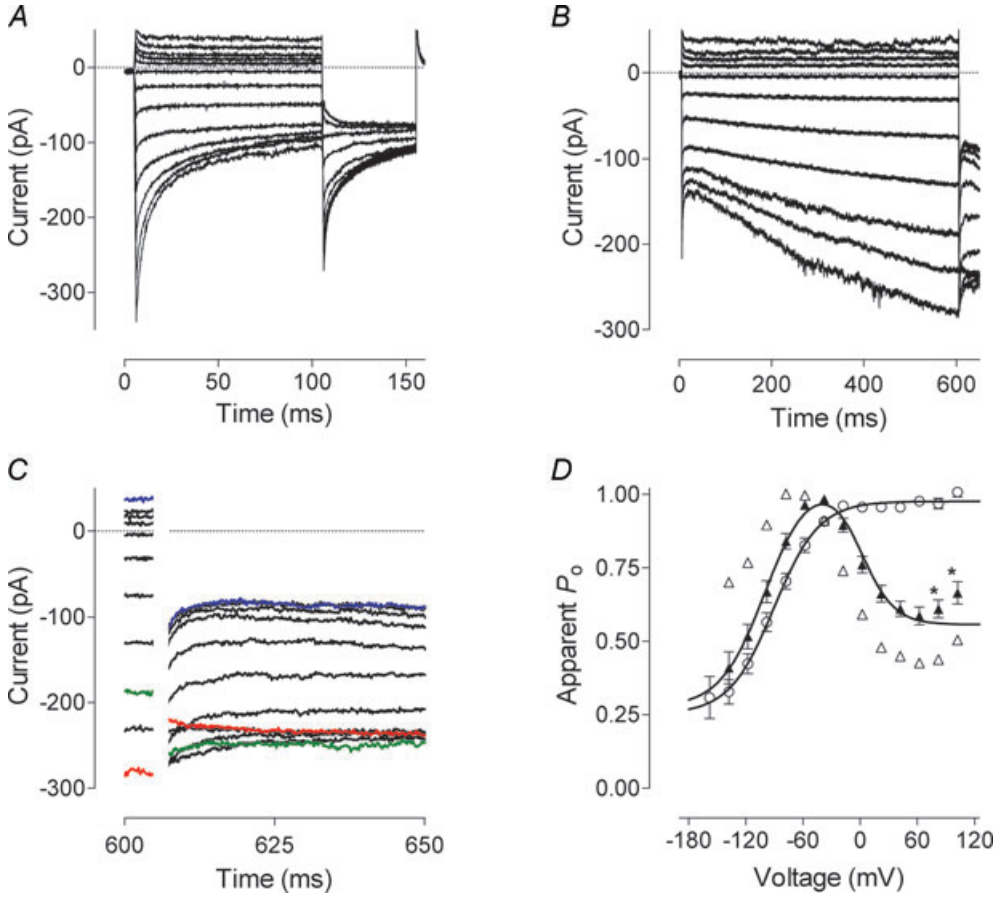


**Figure 6. Voltage dependence of the Orai1/STIM1 mediated $Ca^{2+}$ current**
*A*, current traces obtained in response to 100 ms voltage steps ranging from −158 to 102 mV in 20 mV increments followed by a step to −118 mV. H4IIE cells were transfected with Orai1 and STIM1 at a 1 : 4 molar ratio. *B*, current traces obtained in response to 600 ms voltage steps ranging from −138 to 102 mV in 20 mV increments followed by a step to −118 mV. H4IIE cells were transfected with Orai1 and STIM1 at a 4 : 1 molar ratio. *C*, tail currents shown on panel *B* on a shorter time scale. *D*, apparent open probability of the Orai1 channel obtained by normalising tail currents shown on panels *A* and *B*. Open circles represent averaged data ($n = 6$) obtained in cells expressing inactivating currents. Data from inactivating currents were fitted with a single Boltzmann function (eqn (1), Methods). Filled triangles represent averaged data ($n = 9$) obtained in cells expressing activating currents. Data from activating currents were fitted with a multiple of two Boltzmann functions (eqn (2), Methods). Data points marked with asterisks were excluded from fitting. Open triangles represent the data obtained from cell shown on panel *B*.

In the presence of $Ba^{2+}$, voltage dependence of the inactivating currents was reversed (Fig. 7*A* and *C*). The data points between −100 and 120 mV could be fitted with a single Boltzmann function with the half-maximum activation voltage of −63 mV and the slope corresponding to a gating charge of 1. There was, however, evidence of an opposite voltage dependence at potentials below −100 mV as open probability started to decrease after that point (Fig. 7*C*). It was likely that in a wider range of voltages the open probability would be described by a bell shaped curve; however, it was impossible to obtain a reasonable number of points below −100 mV for proper fitting.

In cells expressing activating $Ca^{2+}$ currents, replacement of $Ca^{2+}$ with $Ba^{2+}$ did not change the shape of the voltage dependence of open probability, but shifted it to more hyperpolarising potentials by approximately 60 mV (Fig. 7*B* and *D*).

### Selectivity in the absence of divalent cations

In the absence of divalent cations in the bath solution the pore of the channel formed by Orai1 peptides becomes permeable to monovalent cations (Mercer *et al.* 2006). In H4IIE cells expressing either activating or inactivating

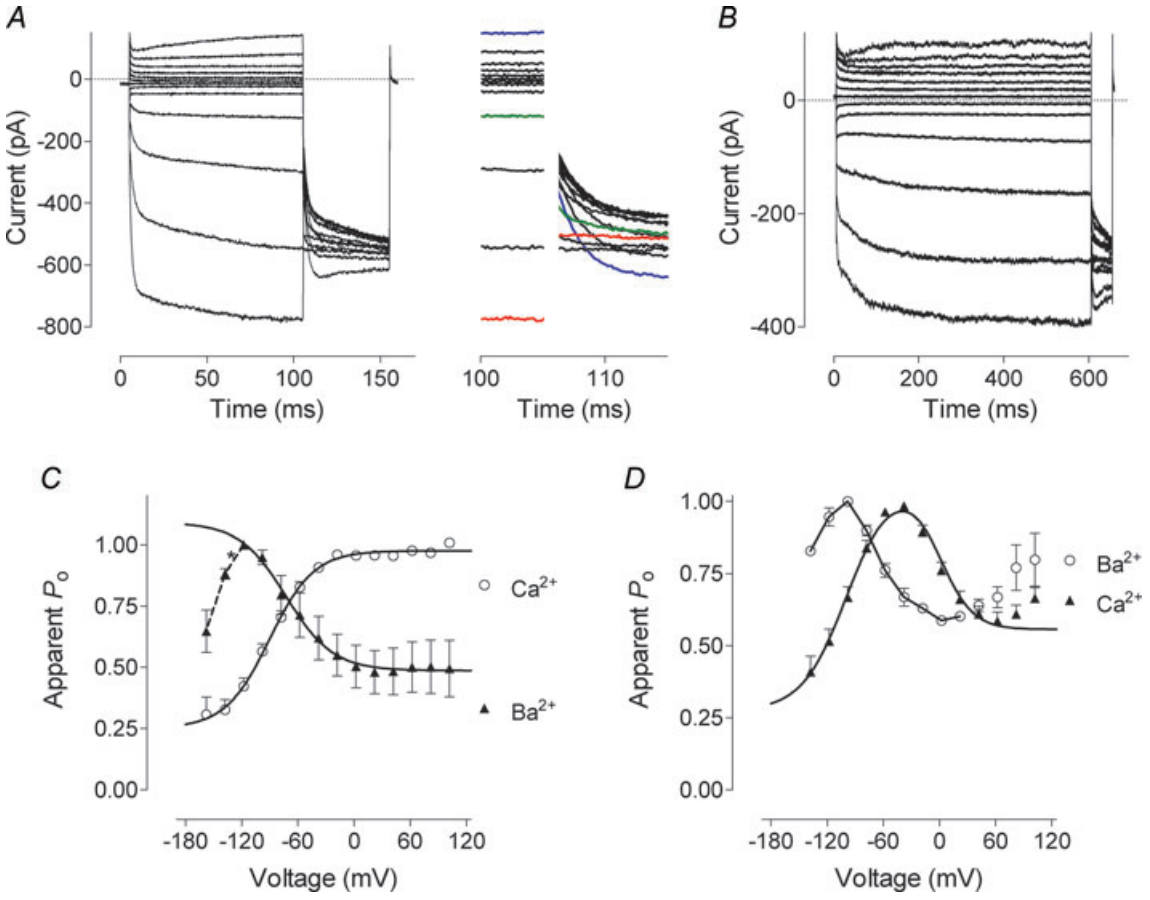


**Figure 7. Voltage dependence of the Orai1/STIM1 mediated current in the presence of $Ba^{2+}$**
*A*, current traces obtained in cells expressing inactivating $Ca^{2+}$ currents (Orai1 and STIM1 at a 1 : 4 molar ratio) in response to 100 ms voltage steps ranging from −158 to 102 mV in 20 mV increments followed by a step to −118 mV. Calcium in the bath solution was replaced with 10 mM $Ba^{2+}$. Inset shows tail currents shown on panel *A* at a shorter time scale. *B*, current traces obtained in cells expressing activating $Ca^{2+}$ currents (Orai1 and STIM1 at a 4 : 1 molar ratio) in response to 600 ms voltage steps ranging from −138 to 102 mV in 20 mV increments followed by a step to −118 mV. $Ca^{2+}$ in the bath solution was replaced with 10 mM $Ba^{2+}$. *C*, apparent open probability of the Orai1 obtained by normalising tail currents shown on panel *A*. Filled triangles represent averaged data ($n = 4$) obtained in the presence of $Ba^{2+}$ in cells expressing inactivating currents. Data were fitted with a single Boltzmann function (eqn (1), Methods). Data points marked with asterisks were excluded from fitting. For comparison, data obtained in the same cells in the presence of $Ca^{2+}$ are shown (open circles). *D*, apparent open probability of the Orai1 obtained by normalising tail currents shown on panel *B*. Open circles represent averaged data ($n = 3$) obtained in the presence of $Ba^{2+}$ in cells expressing activating currents. For comparison, data obtained in the same cells in the presence of $Ca^{2+}$ are shown (filled triangles).

Orai1/STIM1 mediated $Ca^{2+}$ currents, replacement of divalent cations in the bath solution with $Na^+$ caused an approximate fourfold increase of the inward current amplitude (Fig. 8*A*, *B*). In the absence of divalent cations channels formed by Orai1 were more selective for $Na^+$ than $Cs^+$. The relative conductance for $Na^+$ over $Cs^+$ ($G_{Na}/G_{Cs}$) was $4.9 \pm 0.73$ ($n = 4$) and $4.6 \pm 0.57$ ($n = 6$) for activating and inactivating currents, respectively (Fig. 8*B*). Application of the voltage protocol also used in Fig. 6*A* revealed that both activating and inactivating currents lost their voltage dependence in the absence of divalent cations (not shown), and that $Na^+$ currents showed neither activation nor inactivation during steps to negative potentials (Fig. 8*C*).

### Differential effects of 2-APB

2-APB is a known inhibitor of endogenous $I_{SOC}$ and ectopically expressed Orai1/STIM1 mediated current (Gregory *et al.* 2001; Lis *et al.* 2007). It has complex effects on Orai2 and Orai3, but the mechanisms of these effects are not yet understood (Lis *et al.* 2007). In this section we investigated the effects of 2-APB on Orai1/STIM1 mediated currents of different kinetics. While 50 $\mu$M 2-APB blocked 100% of the Orai1/STIM1 mediated current irrespective of the current kinetics, the non-inactivating current showed a marked transient potentiation by 2-APB, while fast inactivating current showed much smaller or no potentiation by 2-APB (Fig. 9*A*, *B*). On average, potentiation of the amplitude of non-inactivating current by 50 $\mu$M 2-APB ($I_{max}/I_{2-APB} = 3.6 \pm 0.65$, $n = 14$) was 6 times stronger than for the inactivating current ($I_{max}/I_{2-APB} = 0.55 \pm 0.13$, $n = 14$, $P < 0.0001$). At the peak of potentiation by 2-APB, the kinetics of the strongly inactivating current was virtually unaffected (Fig. 9*C*). However, if the current showed little inactivation during 200 ms steps to −118 mV in the control solution, it showed strong activation at the peak of potentiation by 2-APB (Fig. 9*C*).

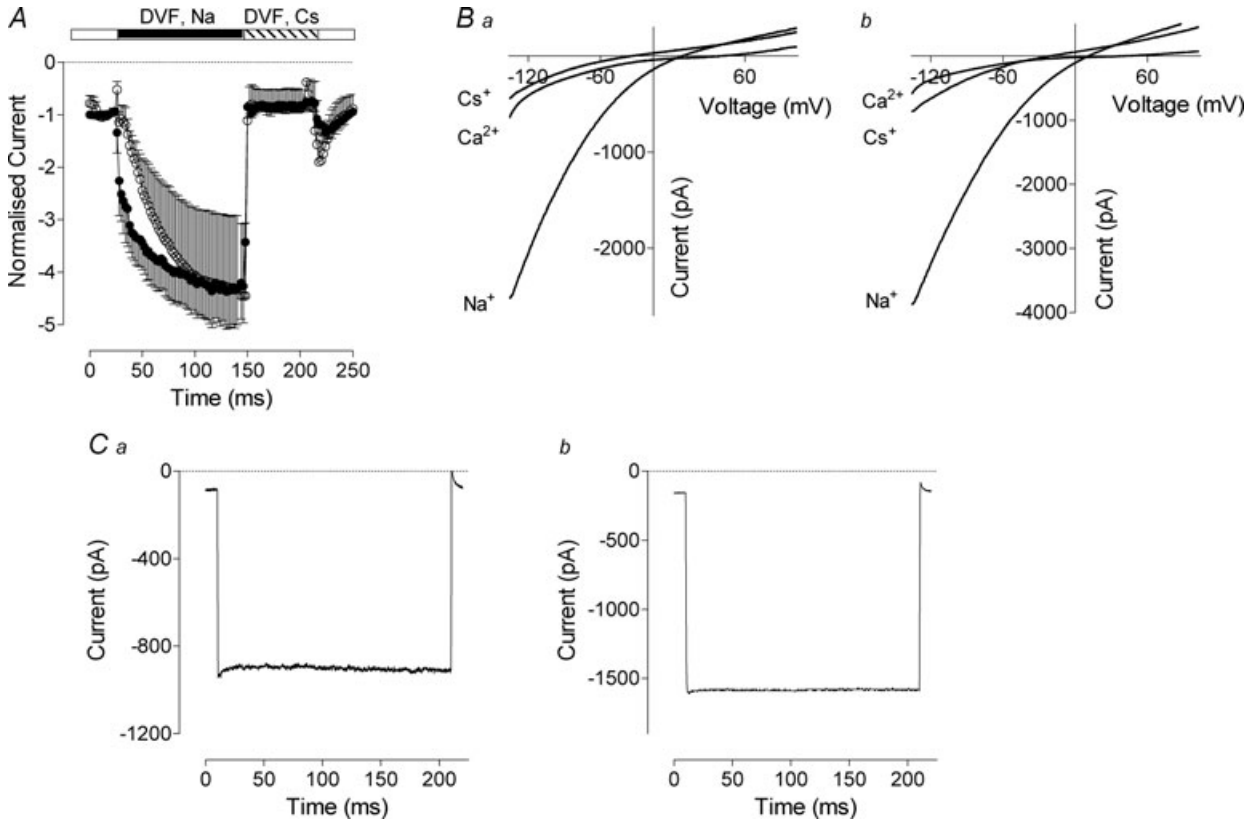


**Figure 8. Orai1/STIM1 mediated cation current in the absence of divalent cations**
*A*, normalised amplitude of the Orai1/STIM1 mediated currents in divalent cation free (DVF) solutions in the presence of $Na^+$ or $Cs^+$ in cells expressing inactivating (filled circles) or activating (open circles) $Ca^{2+}$ currents. Zero-time point corresponds to 60 s after obtaining whole cell configuration. *B*, *I–V* plots of $Ca^{2+}$, $Na^+$ and $Cs^+$ currents recorded in cells expressing inactivating (*a*) and activating (*b*) Orai1/STIM1 mediated $Ca^{2+}$ currents. *C*, current traces recorded in response to 200 ms step to −118 mV in cells expressing inactivating (*a*) and activating (*b*) Orai1/STIM1 mediated $Ca^{2+}$ currents in DVF solution containing $Na^+$. Traces shown on panels *B* and *C* were taken 100–120 s after applying DVF solution in the bath.

To exclude the possibility that 2-APB activates Orai1 directly in the absence of STIM1, we expressed these proteins separately and investigated the effect of 2-APB on the $I_{SOC}$. Expression of Orai1 alone in H4IIE cells did not produce any store-operated current. Moreover, it resulted in a complete suppression of the native $I_{SOC}$ (not shown), as it does in HEK293 cells and rat basophilic leukaemia (RBL) cells (Soboloff *et al.* 2006). Application of 2-APB in H4IIE cells expressing Orai1 alone failed to enhance any current (not shown), suggesting that in the absence of sufficient amounts of STIM1 2-APB does not activate Orai1 even if the stores have been depleted.

## Discussion

The main result of this study is that several key properties of Orai1/STIM1 mediated currents depend on the relative expression levels of STIM1 and Orai1 proteins. Increasing the Orai1 : STIM1 ratio in the transfection mixture from 1 : 4 to 4 : 1 drastically reduces the extent of fast $Ca^{2+}$-dependent inactivation of the current, changes dependence of the whole cell $Ca^{2+}$ conductance on external $Ca^{2+}$, reduces relative $Ba^{2+}$ and $Sr^{2+}$ conductance, changes voltage dependence of the open probability, and increases potentiation by 2-APB.

There are several possible mechanisms which might explain the results of ectopic expression of Orai1 and STIM1. (i) The interaction between Orai1 and STIM1, either direct or through other binding partners, occurs at variable stoichiometry depending on their relative levels of expression. (ii) The stoichiometry of interaction between Orai1 and STIM1 is constant, but there are other binding partners that interact with STIM1 and Orai1. The amount of these other binding partners is

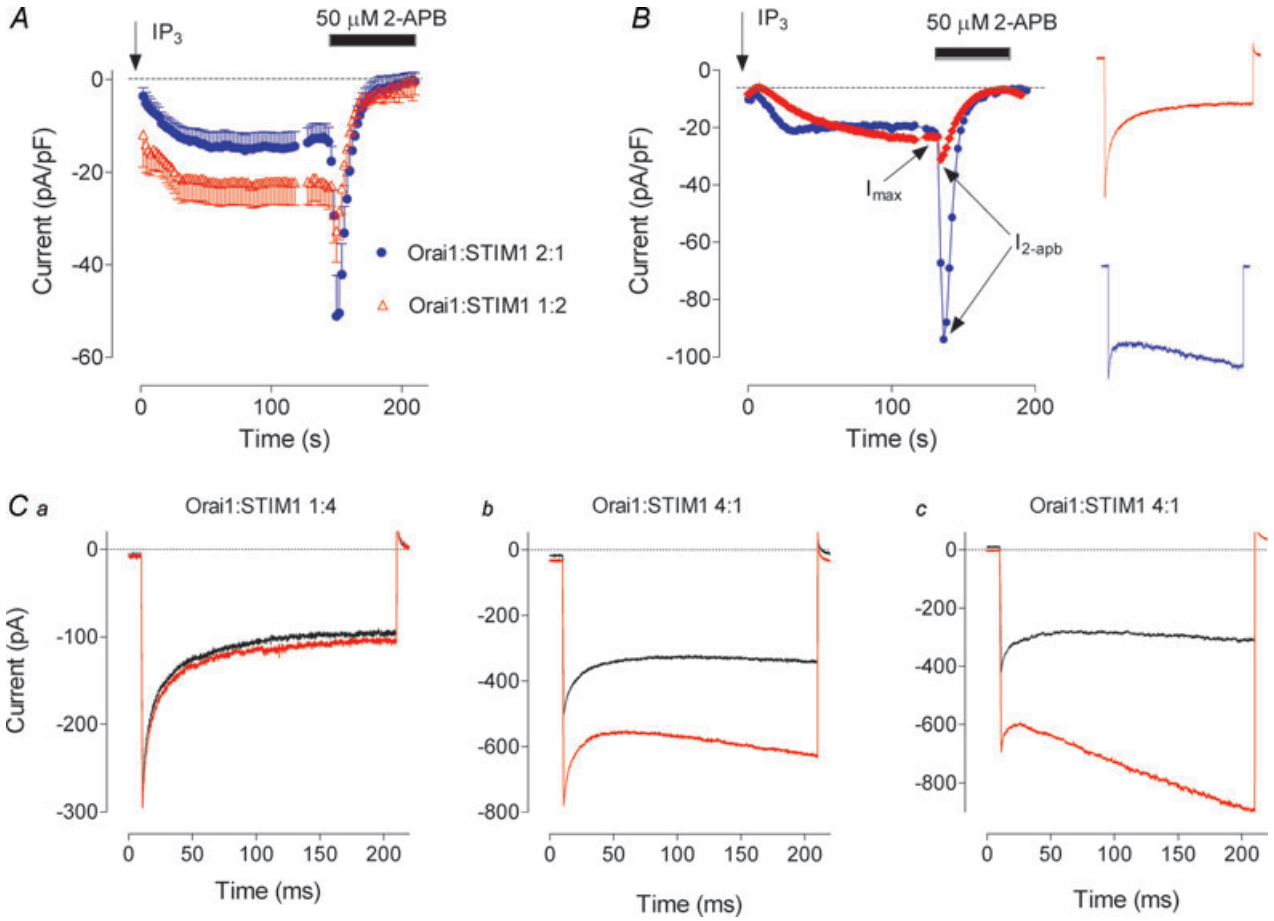


**Figure 9. Effect of 2-APB on Orai1/STIM1 mediated current**
*A*, potentiation and block by 2-APB of Orai1/STIM1 mediated currents recorded under different transfection conditions. Each point represents the amplitude of the current at −118 mV measured from the responses to voltage ramps ranging from −138 mV to 102 mV and applied every 2 s. *B*, examples of 2-APB potentiation of size matched inactivating and non-inactivating Orai1/STIM1 currents. Inset shows current traces from the corresponding cells obtained before application of 2-APB. *C*, dependence of Orai1/STIM1 mediated current kinetics on 2-APB. Examples of current traces obtained in cells expressing different ratios of Orai1 and STIM1 in response to −118 mV steps before application of 2-APB (black) and at the peak of potentiation by 2-APB (red).

limited. High concentrations of either STIM1 or Orai1 not partnered with each other reduce the availability of other binding partners for the functional Orai1/STIM1 complex. (iii) Overexpression of STIM1 and Orai1 modifies the junctional ER and therefore the structure of the microdomains where the functional interaction between them occurs.

Of these mechanisms, the second and the third seem less likely for the following reasons. If the properties of the Orai1/STIM1 currents were dependent on a binding partner present in the cell in limited amounts, which could bind to either STIM1 or Orai1, or both of them, the properties of the current would depend on the absolute amounts, rather then relative amounts, of the expressed proteins. We, however, observed clear dependence of the properties of the Orai1/STIM1 currents on the relative but not absolute expression levels of Orai1 and STIM1. It was possible to record currents with identical kinetics, either inactivating or activating, which differed by up to 10-fold in size, by maintaining the ratio of the plasmids in the transfection mixture but varying their absolute amounts. Furthermore, currents identical in size exhibited opposite voltage dependence if the ratios between Orai1 and STIM1 in the transfection mixture were reversed.

If the levels of expression of either STIM1 or Orai1 were affecting the properties of Orai1/STIM1 mediated current by affecting the properties of junctional ER (Luik *et al.* 2006), this effect would also depend on the absolute but not relative expression levels of these proteins. The only possibility for this mechanism to work would be if there was a particular component in junctional ER that regulated Orai1/STIM1 properties, which was affected by the expression of STIM1 and Orai1 in opposite ways. At present, there are no experimental data to support this idea.

Overall, of all possibilities, variable stoichiometry of binding between Orai1 and STIM1 seems most plausible. There is ample experimental support for the hypothesis that Orai1 and STIM1 interact to form functional complexes that mediate $Ca^{2+}$ entry (Ji *et al.* 2008; Muik *et al.* 2008; Zhang *et al.* 2008). Whether there are any other binding partners in those complexes is still a mater of debate (Li *et al.* 2007; Varnai *et al.* 2007). Recent evidence suggests that ectopically expressed Orai1 form homo-tetramers and each tetramer interacts with two STIM1 peptides (Mignen *et al.* 2008; Penna *et al.* 2008; Zhang *et al.* 2008). Results presented by Zhang *et al.* (2008) are consistent with the notions that stoichiometry of Orai1/STIM1 interaction in the complex varies depending on the relative expression levels of these proteins, and that at least two different stoichiometries are possible.

Regardless of the mechanism, it is clear that relative expression levels of Orai1 and STIM1 affect regulation of the channel by $Ca^{2+}$ coming through the pore. In the absence of divalent cations in the external medium there was no difference between Orai1/STIM1 mediated currents recorded in cells under different transfection conditions. Both inactivation and activation were absent, and the relative sizes of $Na^+$ conductance were identical, as was the selectivity for $Na^+$ over $Cs^+$. This suggests that the relative expression levels of Orai1 and STIM1 do not affect the properties of the pore but rather modify the regulation of open probability of the channel by $Ca^{2+}$.

The difference between inactivating and activating currents in regard to regulation by extracellular $Ca^{2+}$ is evident at both fast and slow time scale. Qualitatively, dependence of the $Ca^{2+}$ conductance on extracellular $Ca^{2+}$ is very similar in cells expressing inactivating and activating Orai1/STIM1 currents. However, compared to cells expressing inactivating currents, cells expressing activating current show significantly larger $Ca^{2+}$ currents at 50 and 100 mM external $Ca^{2+}$, which is consistent with a reduction of feedback inhibition by $Ca^{2+}$.

On a shorter time scale, as expected, kinetics of fast inactivation of Orai1/STIM1 mediated current in cells expressing an excess of STIM1 strongly depended on the external $Ca^{2+}$ concentration between 2 mM and 100 mM. In contrast, in this range of concentrations, kinetics of activation of the current in cells expressing an excess of Orai1 was independent of extracellular $Ca^{2+}$. However, the activation was removed in the absence of the divalent cations in the bath. This suggests that the site responsible for current activation in cells expressing an excess of Orai1 does depend on $Ca^{2+}$, but at a much lower concentration range than the site responsible for fast $Ca^{2+}$-dependent inactivation in cells expressing an excess of STIM1.

The fast $Ca^{2+}$-dependent inactivation of the native $I_{CRAC}$ and the ectopically expressed Orai1/STIM1 current is thought to be due to $Ca^{2+}$ binding to a regulatory site somewhere close to the internal mouth of the pore. Using general assumptions about $Ca^{2+}$ diffusion in the cytoplasmic space it has been suggested that the $Ca^{2+}$ binding site responsible for fast inactivation is likely to be 3–4 nm away from the intracellular mouth of the pore and therefore is likely to be a part of the channel itself (Zweifach & Lewis, 1995*a*). On the other hand, recent investigation of the properties of Orai1 pore mutants suggests that the role of the inactivation gate is played by residues forming the selectivity centre within the pore region of Orai1 (Yamashita *et al.* 2007; Spassova *et al.* 2008). At present it is not yet known if voltage dependence of the current is conferred by the voltage-dependent binding of $Ca^{2+}$ to a regulatory site, or by voltage-dependent movement of a part of the Orai1/STIM1 complex with $Ca^{2+}$ bound to it, or both. While this paper was under review, Park *et al.* (2009) produced convincing evidence that there is a direct binding between STIM1 and Orai1 (Park *et al.* 2009). These authors show that the so-called CRAC activation domain (CAD) of STIM1 binds to both C and N termini of Orai1 and activates $I_{CRAC}$, and that

tetramers of CAD bind to multiple sites on the CRAC channels and create large clusters of Orai1 (Park *et al.* 2009). Moreover, apparently, current activated by CAD lacks fast $Ca^{2+}$-dependent inactivation, but inactivation is restored by increasing the length of C terminus of the peptide (Park *et al.* 2009). This supports the notion that the function of the $Ca^{2+}$ binding site responsible for fast $Ca^{2+}$-dependent inactivation depends on the interaction between STIM1 and Orai1. The results presented in this paper suggest that this interaction between STIM1 and Orai1, and therefore the properties of the regulatory $Ca^{2+}$ binding site(s), or the conformational change within the Orai1/STIM1 complex following $Ca^{2+}$ binding to this site, are affected by the relative expression levels of Orai1 and STIM1. With eight potential binding sites for STIM1 present in Orai1 tetramer, relative expression levels of Orai1 and STIM1 may affect the way the Orai1/STIM1 complex is formed, and therefore, the properties of the regulatory $Ca^{2+}$ binding site. This can explain the observed complex dependence of the channel open probability on voltage and divalent cations.

Lack of inactivation in the presence of $Ba^{2+}$ or $Sr^{2+}$ reported here can be a result of a lower affinity of these cations to the $Ca^{2+}$ binding site involved in inactivation, or their lower efficacy. Similarly, lack of inactivation in cells expressing an excess of Orai1 can be explained by lower affinity of this site for $Ca^{2+}$, or its lower efficacy. Consistent with that, in the cells where Orai1/STIM1 mediated current showed little inactivation at negative potentials, $Ba^{2+}$ had little effect on current kinetics and the apparent open probability curve, just shifting it to more negative potentials, while in cells expressing Orai1/STIM1 current showing strong inactivation, $Ba^{2+}$ abolished most of the inactivation and revealed a different type of gating that opened the channel at negative potentials.

Interestingly, $Ba^{2+}$ has been shown to have different effects on native $I_{CRAC}$ in different cell types. In RBL cells at potentials below −80 mV, $Ba^{2+}$ current through CRAC channels was bigger than $Ca^{2+}$ current, while in Jurkat cells $Ba^{2+}$ current was significantly smaller at all potentials (Hoth, 1995). This difference in $Ba^{2+}$ permeability led to a suggestion that there might be different subtypes of CRAC channels expressed in different cell types. Our data suggest that different cell types that express the same isoforms of Orai and STIM still can have $I_{CRAC}$ with different properties if the ratios of expression of Orai1 and STIM1 are different.

Another salient property of $I_{CRAC}$ is potentiation by lower and inhibition by higher concentrations of 2-APB (Prakriya & Lewis, 2001). It has been suggested that 2-APB potentiates $I_{CRAC}$ by increasing the number of active CRAC channels on the plasma membrane (Prakriya & Lewis, 2006). Potentiation by 2-APB of Orai1/STIM1 mediated currents has been reported in some over-expression studies but not in others (Mercer *et al.* 2006; Lis *et al.* 2007). Here we show that the extent of potentiation of the Orai1/STIM1 current by 2-APB depends on relative levels of expression of Orai1 and STIM1 and correlates with the kinetics of the current. As this potentiation is much greater when the size of the current is limited by the expression of STIM1, one can speculate that 2-APB increases the probability of STIM1 interacting with Orai1, thus increasing the number of active channels on the membrane. With Orai1 in excess this would favour formation of Orai1/STIM1 complexes with fewer STIM1 bound. Alternatively, 2-APB could facilitate opening of the pre-formed channels with fewer STIM1 in the complex. Both these notions are consistent with the observation that potentiation of the amplitude of the Orai1/STIM1 current by 2-APB in cells expressing an excess of Orai1 was accompanied by an increase of activating component of the current recorded at negative voltage steps. Such strong activation of the current at negative potentials could also be achieved in the absence of 2-APB in some cells where, apparently, expression of Orai1 relative to STIM1 was exceptionally high.

In conclusion, we have shown that relative expression levels of Orai1 and STIM1 affect the properties of the ectopically expressed CRAC channels – the fast $Ca^{2+}$-dependent inactivation, relative $Ba^{2+}$ conductance, and potentiation by 2-APB. These data provide an explanation for the previously observed variations in the properties of native $I_{CRAC}$ in different cell types, and for some apparent inconsistencies of over-expression studies where both inactivating and non-inactivating Orai1/STIM1 mediated currents were reported. We believe that relative expression levels of Orai1 and STIM1 affect the stoichiometry of their assembly, and therefore, the properties of the $Ca^{2+}$ binding site responsible for inactivation.

## References

Aromataris EC, Castro J, Rychkov GY & Barritt GJ (2008). Store-operated $Ca^{2+}$ channels and Stromal Interaction Molecule 1 (STIM1) are targets for the actions of bile acids on liver cells. *Biochim Biophys Acta* **1783**, 874–885.

Barry PH (1994). JPCalc, a software package for calculating liquid junction potential corrections in patch-clamp, intracellular, epithelial and bilayer measurements and for correcting junction potential measurements. *J Neurosci Methods* **51**, 107–116.

Feske S, Gwack Y, Prakriya M, Srikanth S, Puppel SH, Tanasa B, Hogan PG, Lewis RS, Daly M & Rao A (2006). A mutation in Orai1 causes immune deficiency by abrogating CRAC channel function. *Nature* **441**, 179–185.

Gregory RB, Rychkov G & Barritt GJ (2001). Evidence that 2-aminoethyl diphenylborate is a novel inhibitor of store-operated $Ca^{2+}$ channels in liver cells, and acts through a mechanism which does not involve inositol trisphosphate receptors. *Biochem J* **354**, 285–290.

Gwack Y, Srikanth S, Feske S, Cruz-Guilloty F, Oh-hora M, Neems DS, Hogan PG & Rao A (2007). Biochemical and functional characterization of Orai proteins. *J Biol Chem* **282**, 16232–16243.

Hoth M (1995). Calcium and barium permeation through calcium release-activated calcium (CRAC) channels. *Pflugers Arch* **430**, 315–322.

Huang GN, Zeng WZ, Kim JY, Yuan JP, Han LH, Muallem S & Worley PF (2006). STIM1 carboxyl-terminus activates native SOC, $I_{CRAC}$ and TRPC1 channels. *Nat Cell Biol* **8**, 1003–U1096.

Ji W, Xu P, Li Z, Lu J, Liu L, Zhan Y, Chen Y, Hille B, Xu T & Chen L (2008). Functional stoichiometry of the unitary calcium-release-activated calcium channel. *Proc Nat Acad Sci U S A* **105**, 13668–13673.

Li ZZ, Lu JZ, Xu PY, Xie XY, Chen LY & Xu T (2007). Mapping the interacting domains of STIM1 and Orai1 in $Ca^{2+}$ release-activated $Ca^{2+}$ channel activation. *J Biol Chem* **282**, 29448–29456.

Liou J, Kim ML, Do Heo W, Jones JT, Myers JW, Ferrell J, James E & Meyer T (2005). STIM is a $Ca^{2+}$ sensor essential for $Ca^{2+}$-store-depletion-triggered $Ca^{2+}$ influx. *Curr Biol* **15**, 1235–1241.

Lis A, Peinelt C, Beck A, Parvez S, Monteilh-Zoller M, Fleig A & Penner R (2007). CRACM1, CRACM2, and CRACM3 are store-operated $Ca^{2+}$ channels with distinct functional properties. *Curr Biol* **17**, 794–800.

Litjens T, Harland ML, Roberts ML, Barritt GJ & Rychkov GY (2004). Fast $Ca^{2+}$-dependent inactivation of the store-operated $Ca^{2+}$ current ($I_{SOC}$) in liver cells: a role for calmodulin. *J Physiol* **558**, 85–97.

Litjens T, Nguyen T, Castro J, Aromataris EC, Jones L, Barritt GJ & Rychkov GY (2007). Phospholipase C-gamma1 is required for the activation of store-operated $Ca^{2+}$ channels in liver cells. *Biochem J* **405**, 269–276.

Luik RM & Lewis RS (2007). New insights into the molecular mechanisms of store-operated $Ca^{2+}$ signaling in T cells. *Trends Mol Med* **13**, 103–107.

Luik RM, Wu MM, Buchanan J & Lewis RS (2006). The elementary unit of store-operated $Ca^{2+}$ entry: local activation of CRAC channels by STIM1 at ER-plasma membrane junctions. *J Cell Biol* **174**, 815–825.

Manji SS, Parker NJ, Williams RT, van Stekelenburg L, Pearson RB, Dziadek M & Smith PJ (2000). STIM1: a novel phosphoprotein located at the cell surface. *Biochim Biophys Acta* **1481**, 147–155.

Mercer JC, DeHaven WI, Smyth JT, Wedel B, Boyles RR, Bird GS & Putney JW (2006). Large store-operated calcium selective currents due to co-expression of Orai1 or Orai2 with the intracellular calcium sensor, STIM1. *J Biol Chem* **281**, 24979–24990.

Mignen O, Thompson JL & Shuttleworth TJ (2008). Orai1 subunit stoichiometry of the mammalian CRAC channel pore. *J Physiol* **586**, 419–425.

Muik M, Frischauf I, Derler I, Fahrner M, Bergsmann J, Eder P, Schindl R, Hesch C, Polzinger B, Fritsch R, Kahr H, Madl J, Gruber H, Groschner K & Romanin C (2008). Dynamic coupling of the putative coiled-coil domain of Orai1 with STIM1 mediates Orai1 channel activation. *J Biol Chem* **283**, 8014–8022.

Park CY, Hoover PJ, Mullins FM, Bachhawat P, Covington ED, Raunser S, Walz T, Garcia KC, Dolmetsch RE & Lewis RS (2009). STIM1 clusters and activates CRAC channels via direct binding of a cytosolic domain to Orai1. *Cell* **136**, 876–890.

Peinelt C, Vig M, Koomoa DL, Beck A, Nadler MJS, Koblan-Huberson M, Lis A, Fleig A, Penner R & Kinet JP (2006). Amplification of CRAC current by STIM1 and CRACM1 (Orai1). *Nat Cell Biol* **8**, 771–773.

Penna A, Demuro A, Yeromin AV, Zhang SL, Safrina O, Parker I & Cahalan MD (2008). The CRAC channel consists of a tetramer formed by STIM-induced dimerization of Orai dimers. *Nature* **456**, 116–120.

Prakriya M, Feske S, Gwack Y, Srikanth S, Rao A & Hogan PG (2006). Orai1 is an essential pore subunit of the CRAC channel. *Nature* **443**, 230–233.

Prakriya M & Lewis RS (2001). Potentiation and inhibition of $Ca^{2+}$ release-activated $Ca^{2+}$ channels by 2-aminoethyldiphenyl borate (2-APB) occurs independently of $IP_3$ receptors. *J Physiol* **536**, 3–19.

Prakriya M & Lewis RS (2006). Regulation of CRAC channel activity by recruitment of silent channels to a high open-probability gating mode. *J Gen Physiol* **128**, 373–386.

Putney JW (2007). New molecular players in capacitative $Ca^{2+}$ entry. *J Cell Sci* **120**, 1959–1965.

Roos J, DiGregorio PJ, Yeromin AV, Ohlsen K, Lioudyno M, Zhang S, Safrina O, Kozak JA, Wagner SL, Cahalan MD, Velicelebi G & Stauderman KA (2005). STIM1, an essential and conserved component of store-operated $Ca^{2+}$ channel function. *J Cell Biol* **169**, 435–445.

Smyth JT, Dehaven WI, Bird GS & Putney JW Jr (2008). $Ca^{2+}$-store-dependent and -independent reversal of STIM1 localization and function. *J Cell Sci* **121**, 762–772.

Soboloff J, Spassova MA, Tang XD, Hewavitharana T, Xu W & Gill DL (2006). Orai1 and STIM reconstitute store-operated calcium channel function. *J Biol Chem* **281**, 20661–20665.

Spassova MA, Hewavitharana T, Fandino RA, Kaya A, Tanaka J & Gill DL (2008). Voltage gating at the selectivity filter of the $Ca^{2+}$ release-activated $Ca^{2+}$ channel induced by mutation of the Orai1 protein. *J Biol Chem* **283**, 14938–14945.

Spassova MA, Soboloff J, He L-P, Xu W, Dziadek MA & Gill DL (2006). STIM1 has a plasma membrane role in the activation of store-operated $Ca^{2+}$ channels. *Proc Natl Acad Sci U S A* **103**, 4040–4045.

Taylor CW (2006). Store-operated $Ca^{2+}$ entry: a STIMulating stOrai. *Trends Biochem Sci* **31**, 597–601.

Varnai P, Toth B, Toth DJ, Hunyady L & Balla T (2007). Visualization and manipulation of plasma membrane-endoplasmic reticulum contact sites indicates the presence of additional molecular components within the STIM1-Orai1 complex. *J Biol Chem* **282**, 29678–29690.

Vig M, Beck A, Billingsley JM, Lis A, Parvez S, Peinelt C, Koomoa DL, Soboloff J, Gill DL, Fleig A, Kinet JP & Penner R (2006*a*). CRACM1 multimers form the ion-selective pore of the CRAC channel. *Curr Biol* **16**, 2073–2079.

Vig M, Peinelt C, Beck A, Koomoa DL, Rabah D, Koblan-Huberson M, Kraft S, Turner H, Fleig A, Penner R & Kinet JP (2006*b*). CRACM1 is a plasma membrane protein essential for store-operated $Ca^{2+}$ entry. *Science* **312**, 1220–1223.

Yamashita M, Navarro-Borelly L, McNally BA & Prakriya M (2007). Orai1 mutations alter ion permeation and $Ca^{2+}$-dependent fast inactivation of CRAC channels: evidence for coupling of permeation and gating. *J Gen Physiol* **130**, 525–540.

Yeromin AV, Zhang SYL, Jiang WH, Yu Y, Safrina O & Cahalan MD (2006). Molecular identification of the CRAC channel by altered ion selectivity in a mutant of Orai. *Nature* **443**, 226–229.

Zhang SL, Kozak JA, Jiang W, Yeromin AV, Chen J, Yu Y, Penna A, Shen W, Chi V & Cahalan MD (2008). Store-dependent and -independent modes regulating $Ca^{2+}$ release-activated $Ca^{2+}$ channel activity of human Orai1 and Orai3. *J Biol Chem* **283**, 17662–17671.

Zhang SL, Yu Y, Roos J, Kozak JA, Deerinck TJ, Ellisman MH, Stauderman KA & Cahalan MD (2005). STIM1 is a $Ca^{2+}$ sensor that activates CRAC channels and migrates from the $Ca^{2+}$ store to the plasma membrane. *Nature* **437**, 902–905.

Zweifach A & Lewis RS (1995*a*). Rapid inactivation of depletion-activated calcium current ($I_{CRAC}$) due to local calcium feedback. *J Gen Physiol* **105**, 209–226.

Zweifach A & Lewis RS (1995*b*). Slow calcium-dependent inactivation of depletion-activated calcium current. *J Biol Chem* **270**, 14445–14451.

## Author contributions

N.S.: conception and design, collection and assembly of data, data analysis and interpretation, manuscript writing; T.L.: conception and design, collection and assembly of data; L.M.: collection and assembly of data, data analysis and interpretation; G.J.B.: conception and design, data interpretation and manuscript writing; G.Y.R.: conception and design, collection of data, data analysis and interpretation, manuscript writing. All authors contributed to final approval of the manuscript. The experiments were conducted in the Laboratory of Cellular Physiology, School of Molecular and Biomedical Science, University of Adelaide.

## Acknowledgments

This work has been supported by the Australian Research Council and NHMRC Australia.